Apoptotic PET Imaging of Rat Pulmonary Fibrosis With [18F]ML-8

Ying Xiong, MM[1], Dahong Nie, BM[1], Shaoyu Liu, PhD[1], Hui Ma, BM[1], Shu Su, BM[1], Aixia Sun, PhD[1], Jing Zhao, MD, PhD[1], Zhanwen Zhang, PhD[1], Xianhong Xiang, MD, PhD[1], and Ganghua Tang, MD, PhD[1]

Abstract

Objective: To investigate the value of 2-(3-[18F]fluoropropyl)-2-methyl-malonic acid ([18F]ML-8) positron emission tomography (PET) imaging of rat pulmonary fibrosis.

Methods: Male Sprague-Dawley rats were divided into 2 groups, including pulmonary fibrosis model group and control group. The rat model was established by an intratracheal instillation of bleomycin (BLM). Control rats were treated with saline. Positron emission tomography/computed tomography (CT) with [18F]ML-8 or 18F-fluorodeoxyglucose ([18F]FDG) was performed on 2 groups. After PET/CT imaging, lung tissues were collected for histologic examination. Data were analyzed and comparisons between 2 groups were performed using Student t test.

Results: Bleomycin-treated rats showed a higher lung uptake of [18F]ML-8 than control rats ($P < .05$). In BLM-treated rats, the lung to muscle relative uptake ratio of [18F]ML-8 was also higher than that of [18F]FDG ($P < .05$). Pathological examination showed overproliferation of fibroblasts and deposition of collagen in lungs from BLM-treated rats. Compared to control rats, BLM-treated rats had higher lung hydroxyproline content ($P < .05$). Immunofluorescence staining indicated more apoptotic cells in BLM-treated rats than those in control rats. Moreover, the apoptosis rate of lung tissues obtained from BLM-treated rats was higher than that from control rats ($P < .05$).

Conclusions: 2-(3-[18F]fluoropropyl)-2-methyl-malonic acid PET/CT could be used for noninvasive diagnosis of pulmonary fibrosis in a rat model.

Keywords

pulmonary fibrosis, diagnosis, PET/CT, [18F]ML-8, [18F]FDG

Introduction

Idiopathic pulmonary fibrosis (IPF) is a progressive and chronic interstitial lung disease with unclear cause. Although inflammation is present in lung tissues of patients with IPF, it doesn't seem to play an important role in the pathogenesis of pulmonary fibrosis as anti-inflammatory treatments have been shown to be ineffective. Idiopathic pulmonary fibrosis is characterized by progressive and irreversible fibrotic changes in the pulmonary parenchyma, including overproliferation of fibroblasts, excessive production of collagens, and other extracellular matrix proteins{Gao, 2016 #1}.[1-6] Patients with IPF have a poor prognosis, with a 5-year mortality rate above 50% and a median survival of 2 to 5 years.[1,5] The current modality of pulmonary fibrosis diagnosis remains high-resolution computed tomography (HRCT) and lung biopsy. However, lung biopsy is an invasive procedure and examines only a small fraction of the lung tissues. High-resolution computed tomography shows the changes of lung density but can't provide functional imaging information of IPF, such as disease activity.[7,8] Compared to HRCT, positron emission tomography (PET)/CT provides both structural and functional imaging

[1] Guangdong Engineering Research Center for Translational Application of Medical Radiopharmaceuticals and Department of Medical Imaging, The First Affiliated Hospital, Sun Yat-sen University, Guangzhou, China

Corresponding Authors:
Ganghua Tang and Xianhong Xiang, Guangdong Engineering Research Center for Translational Application of Medical Radiopharmaceuticals and Department of Medical Imaging, The First Affiliated Hospital, Sun Yat-sen University, Guangzhou 510080, China.
Emails: tangghua@mail.sysu.edu.cn; xxianhong@mail.sysu.edu.cn

information of diseases.[9] In patients with IPF and animal models, the application value of PET/CT has been recently explored, mostly with ^{18}F-fluorodeoxyglucose ([^{18}F]FDG). In these researches, high uptake of [^{18}F]FDG was present in lung tissues of patients with IPF, with a good short-term reproducibility.[3,5,7,8,10-15] However, these studies indicated that lung uptake of [^{18}F]FDG reached a peak value at the early inflammatory phase of pulmonary fibrosis, but the [^{18}F]FDG uptake decreased during the late fibrotic phase.[5,8]

Apoptosis is a mode of cell death that is characterized by nuclear breakup and cell shrinkage, and its deregulation plays a vital role in the pathogenesis of numerous diseases.[16,17] A few recent studies showed that numerous type II pneumocytes in IPF lungs underwent apoptosis and apoptosis of type II pneumocytes plays an important role in the pathogenesis of this disease.[18,19] Molecular imaging of apoptosis may have important implications for noninvasive diagnosis of pulmonary fibrosis or evaluation of antifibrotic treatments. Recently, small molecule radiotracers selectively accumulating in the apoptotic cells have been developed and are used for molecular PET imaging of apoptosis in various preclinical models of apoptosis-related diseases.[20-22] ApoSense family was a novel series of small-molecule probes and it has been designed to detect apoptotic membrane imprint, with selective accumulation in the apoptotic cells.[20] Among these PET tracers, 2-(3-[^{18}F]fluoropropyl)-2-methyl-malonic acid ([^{18}F]ML-8), currently developed by our research group, is a member of ApoSense family and it was demonstrated to specifically bind to apoptotic cells in animal models of apoptosis, such as tumor cell apoptosis induced by antitumor chemotherapy.[21] Thus, we hypothesized that [^{18}F]ML-8 PET/CT could be used for noninvasive diagnosis of pulmonary fibrosis.

The objective of this study was to determine whether PET/CT imaging with [^{18}F]ML-8 could be used for noninvasive visualization of pulmonary fibrosis in the rat pulmonary fibrosis models. Bleomycin (BLM) induction is the most commonly used strategy to generate lung fibrosis in animal models. Preclinical data confirmed that obvious lung fibrosis was detected at the late period of this disease model after a single intratracheal injection of BLM.[4,5] In this article, we present the establishment of the rat pulmonary fibrosis model and quantitative assessment of lung fibrosis in this disease model. The uptake of [^{18}F]ML-8 and detection of apoptosis in fibrotic lung tissues are also investigated.

Materials and Methods

Animals

Male Sprague-Dawley rats weighing 150 to 170 g were used in this study. They were obtained from Laboratory Animal Center of Sun Yat-sen University (Guangzhou, China). They were housed in the specific pathogen free (SPF) animal laboratory and allowed free access to food and water. This study was performed by following the protocol approved by the animal ethical and welfare committee at Sun Yat-sen University.

Establishment of a Rat Model of Pulmonary Fibrosis

Rats were randomly divided into pulmonary fibrosis group and control group (n = 3 per group). We established a rat model of pulmonary fibrosis by means of BLM administration as previously described.[4] Briefly, the pulmonary fibrosis group received a single intratracheal instillation of 5 mg/kg BLM (Bleomycin Hydrochloride for Injection, Nippon Kayaku, Tokyo, Japan) diluted in saline solution. Control group was instilled with the same volume of saline instead. All instillations were performed on rats anesthetized with 2% pentobarbital sodium (0.225 mL/kg). At day 21 after instillation, all rats were used for PET/CT imaging with [^{18}F]ML-8. After PET/CT scans, these rats were sacrificed under deep anesthesia, and lung tissues were collected for further histopathological analysis. Half of the lung was fixed in 4% paraformaldehyde for Masson trichrome staining and terminal deoxynucleotidyl transferase-mediated dUTP nick-end labeling (TUNEL) staining. The remaining half of the lung was prepared for flow cytometry and lung hydroxyproline content measurement.

Small-Animal PET/CT Imaging

Positron emission tomography/CT imaging experiments were performed in control rats and BLM-treated rats using the Inveon small-animal PET/CT scanner (Siemens, Knoxville, Tennessee) at day 21 after instillation (3 rats per group). Preparation of [^{18}F]ML-8 was carried out at our center according to the method described previously.[21] After the weights of rats were recorded, the rats were anesthetized with 2% pentobarbital sodium (0.225 mL/kg). The saline-treated rats and BLM-treated rats were imaged by PET/CT scanner after the tail intravenous injection of [^{18}F]ML-8 solution (37 MBq/kg). For a comparative study, PET/CT with [^{18}F]FDG was also performed on rats after the tail intravenous injection of [^{18}F]FDG solution (37 MBq/kg). Rats were kept fasting for over 4 hours before injection of [^{18}F]FDG. Anesthetized rats were placed in the supine position in the small-animal PET/CT scanner. Positron emission tomography/CT imaging was performed for 60 minutes after [^{18}F]ML-8 or [^{18}F]FDG injection and stored digitally. Imaging acquisition started with a low-dose CT scan and followed by a 10-minute PET scan immediately. The CT scan was used for localization of the lesion site and attenuation correction. The PET acquisitions were reconstructed using the 2-dimensional ordered-subset expectation maximum iterative reconstruction method. For each PET image, the regions of interest (ROIs) were drawn over the lesion site of lung and muscle by using Inveon Research Workplace 4.1 software. Mean radioactivity within each ROI was measured to quantify the uptake of [^{18}F]ML-8 expressed as percentage injected dose per gram of tissue (%ID/g).

Histopathological Examination

Masson trichrome staining was performed to observe the pathological changes in lung tissues of rats as previously

described.[5] Briefly, lung tissues were fixed in 4% paraformaldehyde, embedded in paraffin, and cut into 4-μm-thick sections. The obtained lung tissue sections were stained with Masson trichrome staining for light microscopic examination. The degree of pulmonary fibrosis was scored according to the method described by Ashcroft et al.[23] Fibrotic changes of each lung were measured by calculating the mean of the pathologic scores on 6 different fields (magnification × 40). The fibrosis classification was as follows: normal lung (grade 0), minimal fibrous thickening of alveolar or bronchiolar walls (grade 1), moderate thickening of walls without obvious damage to lung architecture (grade 3), increased fibrosis with definite damage to lung structure and formation of fibrous bands or small fibrous masses (grade 5), severe distortion of structure and large fibrous areas (grade 7), and total fibrous obliteration of the field (grade 8).

Measurement of Lung Collagen Content

Hydroxyproline is a specific component of collagen and a marker of fibrosis.[4,5] The measurement of hydroxylproline (HYP) level can be used to estimate the content of collagen in the lung tissues. Lung hydroxyproline content was measured using an HYP kit (Sigma-Aldrich, Burlington, Vermont) according to the manufacturer's instructions. Briefly, 10 mg of lung tissues was homogenized in 100 μL of water and then hydrolyzed in 100 μL of concentrated hydrochloric acid ($\sim$ 12 M) for 3 hours at 120°C. Ten μL of supernatant was transferred to a 96 well plate and then evaporated to dryness. After the addition of 100 μL of the chloramine T/oxidation buffer and 100 μL of the diluted 4-(Dimethylamino)benzaldehyde reagent, the absorbance of each sample at 560 nm was measured. Hydroxyproline content in lung tissues was expressed as micrograms of HYP per milligram wet lung tissue (μg/mg).

Immunofluorescence Staining

Immunofluorescence staining was used to evaluate the extent of apoptosis in lung tissues. Cell apoptosis was confirmed by the TUNEL) method using the in situ cell death detection kit (Roche, Mannheim, Germany) according to the manufacture's protocol. The obtained lung tissue sections (4 μm thick) were collected and stained with TUNEL and 4',6-diamidino-2-phenylindole probe to observe the presence of apoptotic cells in the lung tissues. Observed under a fluorescence microscope, the apoptotic cells of lung tissues were stained in green.

Flow Cytometry Analysis

Flow cytometry is used to quantitatively determine the percentage of apoptotic cells within lung tissues. Lungs were collected, rinsed with PBS, minced, enzymatically digested and filtered through a 200-mesh nylon net. After centrifugation, apoptosis rates of cells were measured using a FITC Annexin V apoptosis detection kit (Becton Dickson, Franklin Lakes, New Jersey) according to manufacturer's instructions, and then analyzed by flow cytometry (Guava easyCyte; EMD Millipore

Corporation, Odessa, Texas). Finally, all data were processed with guavaSoft 1.0.

Statistical Analysis

Quantitative data were expressed as mean (standard deviation [SD]). Significance was determined using the 2-tailed Student t test for single comparison. All analyses were performed by Prism software (version 6.0; GraphPad, La Jolla, California) and SPSS software (version 20.0; SPSS Inc, IBM, Armonk, New York), and values of $P < .05$ were considered indicative of a statistically significant difference.

Results

General Situation of Rats

At day 21 after administration of saline or BLM, rats' mental status, appetite, coat color, and body weight were monitored. In the control group, rats had a good appetite and their body weight increased significantly. They were active and their fur was bright and smooth. Compared to control group, food intake of BLM-treated rats was reduced and their body weight was decreased. Moreover, rats in the BLM group were inactive and their fur was gloomy and dark. Compared to control rats, BLM-treated rats had worse lung function. Bleomycin-treated rats had symptoms of cough and shortness of breath. Altogether, the situation of rats in the BLM group was worse than that in the control group.

2-(3-[^{18}F]Fluoropropyl)-2-Methyl-Malonic Acid PET/CT Imaging

In order to investigate whether PET/CT imaging with [^{18}F]ML-8 could be used for noninvasive diagnosis of the rat pulmonary fibrosis model, the uptake of [^{18}F]ML-8 in lung tissues was analyzed for comparisons between 2 groups at indicated time points. At day 21 after instillation, CT images showed strong alterations with areas of lung consolidations in BLM-treated rats. In the control group, CT scans of lung tissues were normal with no evidence of abnormal pulmonary density. The examination of PET/CT images demonstrated that [^{18}F]ML-8 accumulated selectively in the fibrotic areas of lung tissues in BLM-treated rats, as compared to control rats (Figure 1A). Compared to control rats, a significant increase in [^{18}F]ML-8 uptake of lung tissues was observed in BLM-treated rats at day 21 (0.09% [0.01%] ID/g vs 0.79% [0.06%] ID/g, respectively; $P < .05$; Figure 1B). Furthermore, the ratios of lung versus muscle (lung/background ratio) were also analyzed for comparisons between 2 groups. At day 21, the lung to muscle relative uptake ratio of [^{18}F]ML-8 in the BLM group was higher than that in the control group (3.85 [0.23] vs 1.42 [0.14], respectively; $P < .05$; Figure 1C). As a typical PET radiotracer for apoptosis imaging, the [^{18}F]ML-8 uptake in BLM group showed a strong positive correlation with apoptosis rate ($R^2 = 0.9823$, $P < .01$; Figure 1D) and degree of pulmonary fibrosis (Ashcroft score; $R^2 = 0.9038$, $P < .05$; Figure 1E).

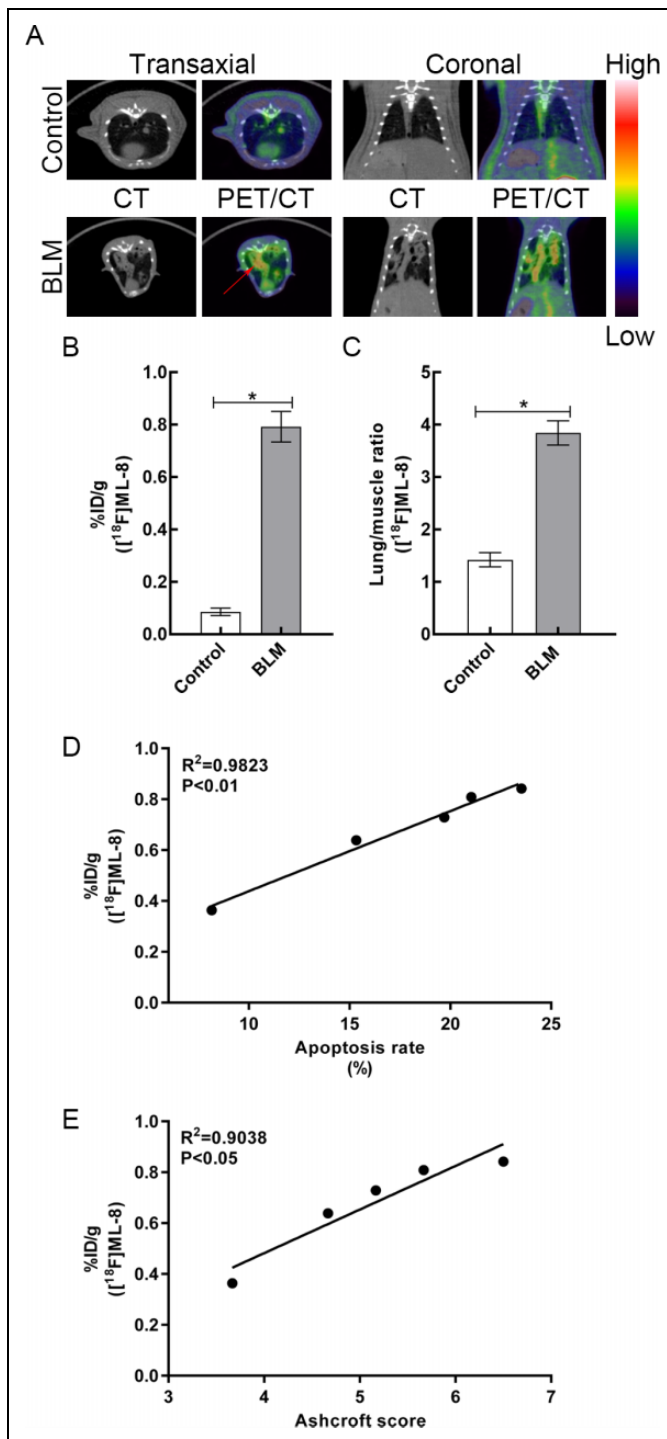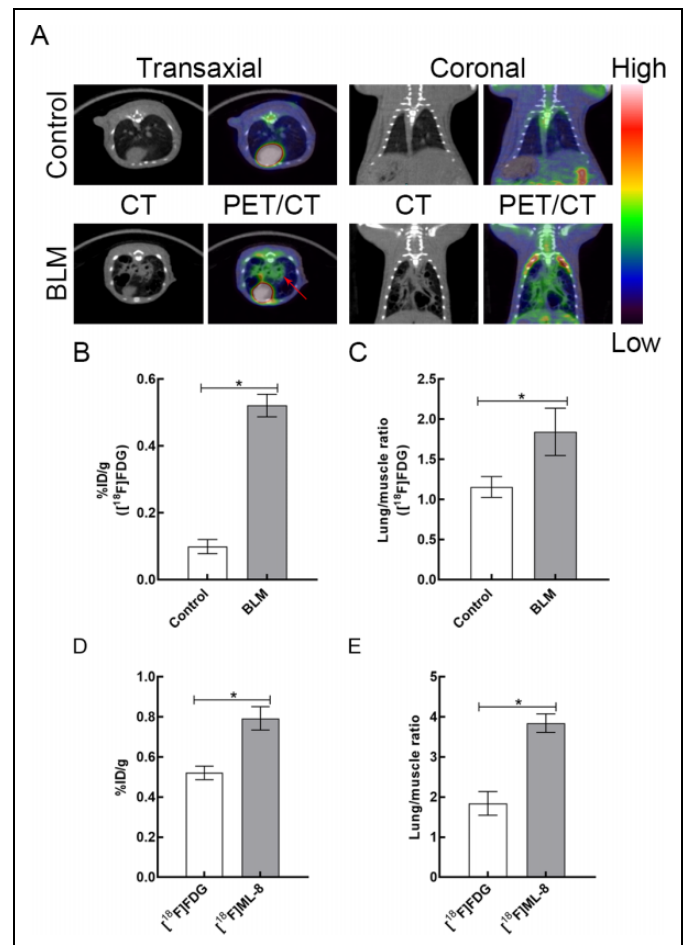**Figure 1.** A, Representative [^{18}F]ML-8 PET/CT images in control and BLM groups at day 21 after instillation. (The red arrows indicate fibrotic lung tissues.) B, The lung uptake of [^{18}F]ML-8 in control and BLM groups at 1 hour after injection. C, The lung versus muscle uptake ratio of [^{18}F]ML-8 in 2 groups. D, Correlation between apoptosis rate and [^{18}F]ML-8 uptake. E, Correlation between degree of pulmonary fibrosis (Ashcroft score) and [^{18}F]ML-8 uptake. Data are reported as mean (standard deviation; N = 3 for each group).*P < .05. BLM indicates bleomycin; CT, computed tomography; [^{18}F]ML-8, 2-(3-[^{18}F]fluoropropyl)-2-methyl-malonic acid; PET, positron emission tomography.

Figure 2. A, Representative [^{18}F]FDG PET/CT images in control and BLM groups at day 21 after instillation. (The red arrows indicate fibrotic lung tissues.) B, The lung uptake of [^{18}F]FDG in control and BLM groups at 1 hour after injection. C, The lung versus muscle uptake ratio of [^{18}F]FDG in 2 groups. D, The uptake of fibrotic lung tissues between [^{18}F]FDG and [^{18}F]ML-8 in the BLM group. E, Bar chart shows difference in the uptake ratio (lung versus muscle) between [^{18}F]ML-8 PET and [^{18}F]FDG PET at day 21 after instillation. Data are reported as mean (standard deviation; N = 3 for each group).*P < .05. BLM indicates bleomycin; CT, computed tomography; [^{18}F]FDG, ^{18}F-fluorodeoxyglucose; [^{18}F]ML-8; 2-(3-[^{18}F]fluoropropyl)-2-methyl-malonic acid; PET, positron emission tomography.

^{18}F-Fluorodeoxyglucose PET/CT Imaging

As shown in Figure 2A, [^{18}F]FDG PET/CT was conducted on control rats and BLM-treated rats. Compared to control group, BLM group showed a significantly higher [^{18}F]FDG uptake (0.10% [0.02%] ID/g vs 0.52% [0.03%] ID/g, respectively; P < .05; Figure 2B) and a higher uptake ratio of lung versus muscle (1.16 [0.13] vs 1.84 [0.30], respectively; P < .05; Figure 2C). Furthermore, the uptake of fibrotic lung tissues and the uptake ratio (lung versus muscle) were also analyzed for comparisons between [^{18}F]ML-8 PET/CT and [^{18}F]FDG PET/CT at day 21 after instillation. The uptake between [^{18}F]FDG and [^{18}F]ML-8 in the BLM group has significant difference (0.52% [0.03]% ID/g vs 0.79% [0.06]% ID/g, respectively; P < .05;
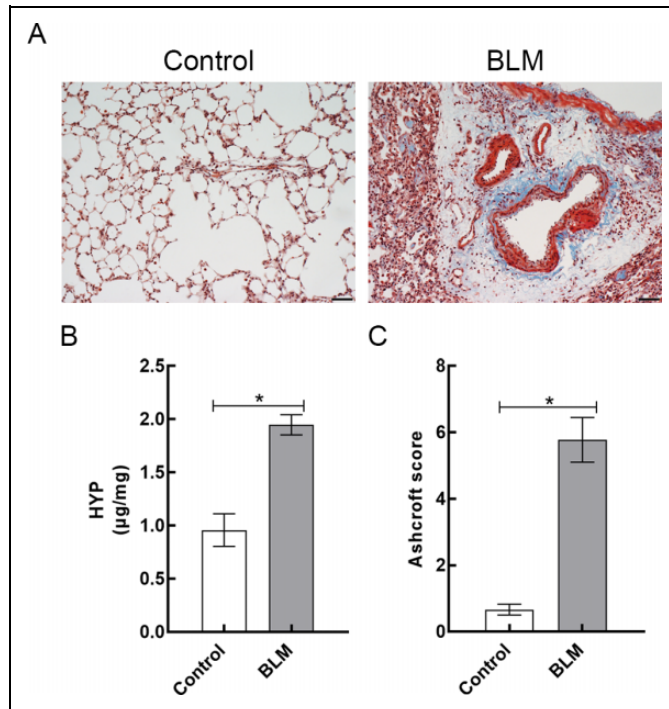
Figure 3. A, Representative lung sections stained with Masson trichrome (magnification, × 200) of control rats and BLM-treated rats. B, Lung HYP content in control and BLM groups. C, Ashcroft scores of 2 groups were measured at day 21 after instillation. Data are reported as mean (standard deviation; N = 3 for each group). *P < .05. Scale bars = 50 μm. BLM indicates bleomycin; HYP, hydroxylproline.

Figure 2D). In the BLM group, the uptake ratio of [^{18}F]ML-8 was also significantly higher than that of [^{18}F]FDG (3.85 [0.23] vs 1.84 [0.30], respectively; $P < .05$; Figure 2E).

Assessment of Pulmonary Histopathology

According to the Masson trichrome staining, rats in the control group had normal alveolar structure and no pathological changes. In the BLM group, significant pulmonary fibrosis was observed in lung tissues, including overproliferation of fibroblasts, excessive deposition of collagens, thickening of alveolar septa, and destruction of alveolar structure (Figure 3A). At day 21 after instillation, lung HYP content was measured from 2 groups to assess their collagen content.[4,5] Lung HYP content in the BLM group was significantly higher than that in the control group (1.95 [0.10] μg/mg vs 0.96 [0.15] μg/mg, respectively; $P < .05$; Figure 3B). Based on the Ashcroft method, the degree of pulmonary fibrosis was evaluated statistically.[23] Compared to control rats, BLM-treated rats showed a higher degree of pulmonary fibrosis (0.67 [0.17] vs 5.78 [0.67], respectively; $P < .05$; Figure 3C).

Apoptosis Detection

For detection of apoptotic cells in lung tissues obtained from 2 groups, lung sections were collected and TUNEL assay was performed. As shown in Figure 4A, compared to control group,
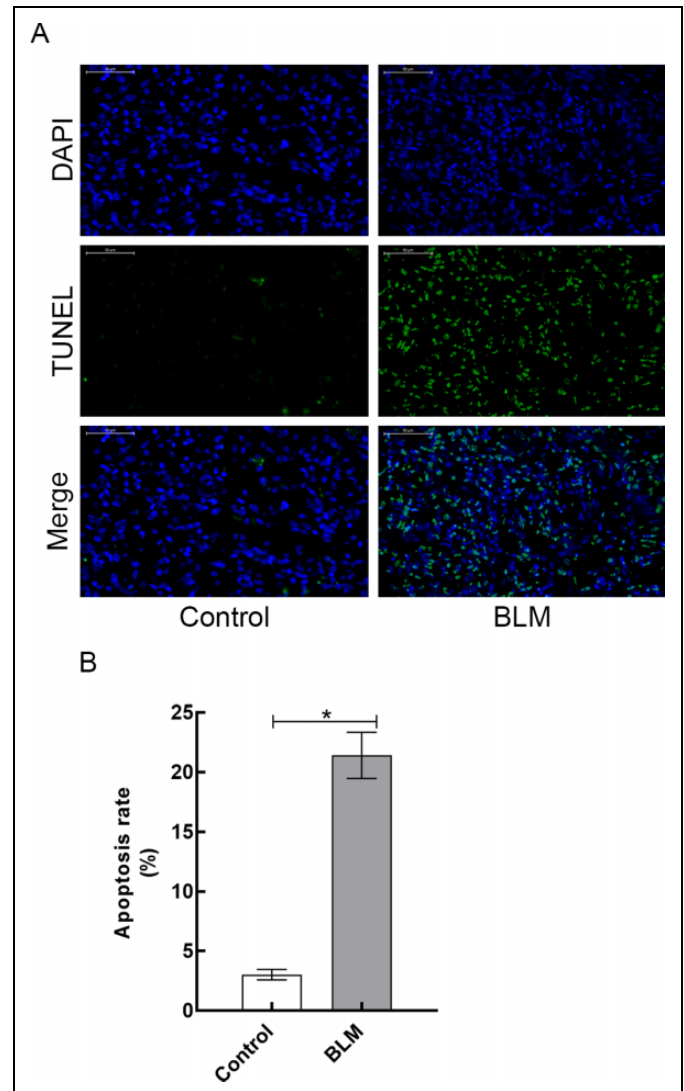

Figure 4. A, Terminal deoxynucleotidyl transferase-mediated dUTP nick-end labeling (TUNEL) staining analysis of lung tissues harvested from control and BLM groups. B, Apoptosis rate of lung tissues in control and BLM groups. Data are reported as mean (standard deviation; N = 3 for each group).*P < .05. Scale bars = 50 μm. BLM indicates bleomycin.

more apoptotic cells were observed in the lung tissues of BLM group. Furthermore, the apoptosis rates of lung tissues in 2 groups were quantitatively determined by flow cytometry. Compared to control rats, apoptosis rate of lung tissues in BLM-treated rats was significantly higher (3.02% [0.44%] vs 21.42% [1.94%], respectively; $P < .05$; Figure 4B).

Discussion

Idiopathic pulmonary fibrosis is a chronic, progressive, interstitial fibrotic lung disease with a worse mortality rate than many cancers.[24,25] The etiology of IPF has not been clearly uncovered. Idiopathic pulmonary fibrosis is induced by a variety of environmental and genetic factors, which result in

repetitive type II alveolar epithelial cell injury and abnormal lung repair processes, proliferation of fibroblasts, and excessive accumulation of extracellular matrix proteins, which finally leads to destruction of the lung architecture and severe insufficient pulmonary functions.[5,26,27] Today, HRCT is used for noninvasive imaging diagnosis of pulmonary fibrosis and the assessment of response to antifibrotic treatment in patients with IPF.[28] Although HRCT can observe abnormal pulmonary density, it can't provide functional imaging information of this disease.[13] Therefore, validated noninvasive methods to accurately diagnose IPF are crucial for improving patient care and evaluating the effect of antifibrotic therapy.

The aim of this study was to investigate the application value of [18F]ML-8 PET/CT to diagnose IPF in a rat model. In this study, the rat pulmonary fibrosis model was established by intratracheal injection of BLM, which was shown to induce lung fibrosis in a wide variety of experimental animals. In the previous studies, neutrophilic and lymphocytic alveolitis occurred in lung tissues within the first week after BLM administration, and then alveolar inflammatory cells were cleared, fibroblast proliferation and excessive production of extracellular matrix occurred at the later period of this disease model. The induction of a strong fibrotic response was detected biochemically and histologically by day 14, with maximal fibrotic responses noted around days 21 to 28.[5,29] In this study, Masson trichrome staining helped to confirm the pathologic process of pulmonary fibrosis. The alveoli of BLM-treated rat was structurally disordered, with overproliferation of alveolar septal fibroblasts, deposition of collagens, and alveolar architectural destruction with honeycombing areas. According to Masson trichrome staining, fibrosis score of lung tissues in the BLM group was significantly higher than that in the control group. In addition, a significant increase in lung HYP content was observed in BLM-treated rats, as compared to control rats. These results demonstrated that the rat pulmonary fibrosis model was successfully established.

The mechanisms of pulmonary fibrosis are still unclear. Several recent researches describe the crucial role of apoptosis in the pathogenesis of pulmonary fibrosis.[18,19] Researches on normal lung tissues show that type II alveolar epithelial cells cover 7% of the alveolar surface and represent 16% of the total alveolar cells. The synthesis and secretion of surfactant is the function of type II pneumocytes. Surfactant is a complex of proteins and phospholipids and it is capable of maintaining alveolar stability by decreasing surface tension of the air–tissue interface. Recent study demonstrated that apoptosis of type II pneumocytes occurred in normal alveoli of patients with IPF and could be crucial for the pathogenesis of this disease. In this study, it indicated that apoptosis of type II pneumocytes could hinder the synthesis of surfactant, causing alveolar collapse, allowing an inflammatory reaction in the lung tissues, and eventually leading to the development of pulmonary fibrosis.[18] In our research, the presence of apoptotic cells in lung sections was determined by TUNEL staining and flow cytometry. Our results demonstrated that the amount of apoptotic cells in the lungs of BLM group was more than that in the control group.

Flow cytometry results showed that BLM-treated rats showed higher apoptosis rate of lung tissues than control rats. We then proposed that selective accumulation of [18F]ML-8 in the pulmonary fibrotic tissues could be mainly contributed to apoptosis of type II pneumocytes, but needed to be further confirmed. Furthermore, accumulation of [18F]ML-8 in the lung tissues showed a strong positive correlation with apoptosis rate and degree of pulmonary fibrosis in a rat model. Therefore, we concluded that apoptotic PET imaging with [18F]ML-8 could be used for noninvasive diagnosis of pulmonary fibrosis in a rat model.

Apoptosis is a complicated process with apoptotic membrane imprint occurring in the early phase. A characteristic feature of the ApoSense family is that they can detect apoptotic membrane imprint and selectively target cells undergoing apoptosis finally.[20] 2-(3-[18F]fluoropropyl)-2-methyl-malonic acid is a member of ApoSense family and it was designed to selectively bind to the altered cell membrane and finally accumulate in the apoptotic cells. As reported in the previous study, [18F]ML-8 with low molecular weight can be used with PET/CT to detect merely the apoptotic regions of tumors after antitumor chemotherapy.[21] In this study, compared to control group, PET data showed that there was a significant increased uptake of [18F]ML-8 in the lung tissues obtained from BLM-treated rats and fibrotic areas were more visible with high contrast to muscle in the BLM group. The PET/CT fusion images showed that the maximal [18F]ML-8 uptake was concentrated in fibrotic areas of the lung tissues, which were characterized by the reticulation and honeycombing. Furthermore, fibrotic areas were more visible with high contrast to muscle in the [18F]ML-8 PET images, compared to [18F]FDG PET images. Histopathological examination of the lung sections obtained from BLM- and saline-treated rats injected with [18F]ML-8 showed that this tracer accumulated only in fibrotic areas, in which the number of apoptotic cells increased significantly. Altogether, these results indicated that PET/CT imaging of [18F]ML-8 could be used for noninvasive diagnosis of pulmonary fibrosis in a rat model.

This study has several limitations. This study used a pulmonary fibrosis model induced by intratracheal injection of BLM in rat lungs. Although this model is the most commonly used, it may not reflect all types of pulmonary fibrosis, such as radiation-induced pulmonary fibrosis. Therefore, further studies of [18F]ML-8 PET/CT imaging in other types of lung fibrosis models and clinical experiments may be required to further illustrate the potential of [18F]ML-8 PET/CT for pulmonary fibrosis imaging.

Conclusions

This study demonstrated that [18F]ML-8 PET/CT could be used to noninvasively diagnose pulmonary fibrosis in a rat model. Further animal studies and clinical experiments are necessary to validate this application of [18F]ML-8 PET/CT for diagnosis of pulmonary fibrosis.

Authors' Note

Authors Ying Xiong and Dahong Nie contributed equally to this work.

Declaration of Conflicting Interests

Funding

References

1. Gao Q, Li Y, Pan X, Yuan X, Peng X, Li M. Lentivirus expressing soluble ST2 alleviates bleomycin-induced pulmonary fibrosis in mice. *Int Immunopharmacol*. 2016;30:188–193. doi:10.1016/j.intimp.2015.11.015.

2. Li XX, Jiang DY, Huang XX, Guo SL, Yuan W, Dai HP. Toll-like receptor 4 promotes fibrosis in bleomycin-induced lung injury in mice. *Genet Mol Res*. 2015;14(4):17391–17398. doi:10.4238/2015.December.21.8.

3. Lavalaye J, Grutters JC, van de Garde EM, et al. Imaging of fibrogenesis in patients with idiopathic pulmonary fibrosis with cis-4-[(18)F]-Fluoro-L: -proline PET. *Mol Imaging Biol*. 2009;11(2):123–127. doi:10.1007/s11307-008-0164-1.

4. Zhang K, Si XP, Huang J, et al. Preventive effects of Rhodiola rosea L. on bleomycin-induced pulmonary fibrosis in rats. *Int J Mol Sci*. 2016;17(6):E879. doi:10.3390/ijms17060879.

5. Bondue B, Sherer F, Van Simaeys G, et al. PET/CT with 18F-FDG- and 18F-FBEM-labeled leukocytes for metabolic activity and leukocyte recruitment monitoring in a mouse model of pulmonary fibrosis. *J Nucl Med*. 2015;56(1):127–132. doi:10.2967/jnumed.114.147421.

6. Raghu G, Anstrom KJ, King TE Jr, et al. Prednisone, azathioprine, and N-acetylcysteine for pulmonary fibrosis. *N Engl J Med*. 2012;366(21):1968–1977. doi:10.1056/NEJMoa1113354.

7. Ambrosini V, Zompatori M, De Luca F, et al. 68Ga-DOTANOC PET/CT allows somatostatin receptor imaging in idiopathic pulmonary fibrosis: preliminary results. *J Nucl Med*. 2010;51(12):1950–1955. doi:10.2967/jnumed.110.079962.

8. Jones HA, Schofield JB, Krausz T, Boobis AR, Haslett C. Pulmonary fibrosis correlates with duration of tissue neutrophil activation. *Am J Respir Crit Care Med*. 1998;158(2):620–628. doi:10.1164/ajrccm.158.2.9711075.

9. Blodgett TM, Meltzer CC, Townsend DW. PET/CT: form and function. *Radiology*. 2007;242(2):360–385. doi:10.1148/radiol.2422051113.

10. El-Chemaly S, Malide D, Yao J, et al. Glucose transporter-1 distribution in fibrotic lung disease: association with [(1)(8)F]-2-fluoro-2-deoxyglucose-PET scan uptake, inflammation, and neovascularization. *Chest*. 2013;143(6):1685–1691. doi:10.1378/chest.12-1359.

11. Groves AM, Win T, Screaton NJ, et al. Idiopathic pulmonary fibrosis and diffuse parenchymal lung disease: implications from initial experience with 18F-FDG PET/CT. *J Nucl Med*. 2009;50(4):538–545. doi:10.2967/jnumed.108.057901.

12. Meissner HH, Soo Hoo GW, Khonsary SA, Mandelkern M, Brown CV, Santiago SM. Idiopathic pulmonary fibrosis: evaluation with positron emission tomography. *Respiration*. 2006;73(2):197–202. doi:10.1159/000088062.

13. Umeda Y, Demura Y, Ishizaki T, et al. Dual-time-point 18F-FDG PET imaging for diagnosis of disease type and disease activity in patients with idiopathic interstitial pneumonia. *Eur J Nucl Med Mol Imaging*. 2009;36(7):1121–1130. doi:10.1007/s00259-009-1069 -1.

14. Win T, Lambrou T, Hutton BF, et al. 18F-Fluorodeoxyglucose positron emission tomography pulmonary imaging in idiopathic pulmonary fibrosis is reproducible: implications for future clinical trials. *Eur J Nucl Med Mol Imaging*. 2012;39(3):521–528. doi:10.1007/s00259-011-1986-7.

15. Win T, Screaton NJ, Porter J, et al. Novel positron emission tomography/computed tomography of diffuse parenchymal lung disease combining a labeled somatostatin receptor analogue and 2-deoxy-2[18F]fluoro-D-glucose. *Mol Imaging*. 2012;11(2):91–98.

16. Taylor RC, Cullen SP, Martin SJ. Apoptosis: controlled demolition at the cellular level. *Nat Rev Mol Cell Biol*. 2008;9(3):231–241. doi:10.1038/nrm2312.

17. Kadirvel M, Fairclough M, Cawthorne C, et al. Detection of apoptosis by PET/CT with the diethyl ester of [(1)(8)F]ML-10 and fluorescence imaging with a dansyl analogue. *Bioorg Med Chem*. 2014;22(1):341–349. doi:10.1016/j.bmc.2013.11.019.

18. Barbas-Filho JV, Ferreira MA, Sesso A, Kairalla RA, Carvalho CR, Capelozzi VL. Evidence of type II pneumocyte apoptosis in the pathogenesis of idiopathic pulmonary fibrosis (IFP)/usual interstitial pneumonia (UIP). *J Clin Pathol*. 2001;54(2):132–138.

19. Fine A, Janssen-Heininger Y, Soultanakis RP, Swisher SG, Uhal BD. Apoptosis in lung pathophysiology. *Am J Physiol Lung Cell Mol Physiol*. 2000;279(3):L423–L427.

20. Reshef A, Shirvan A, Akselrod-Ballin A, Wall A, Ziv I. Small-molecule biomarkers for clinical PET imaging of apoptosis. *J Nucl Med*. 2010;51(6):837–840. doi: 10.2967/jnumed.109.063917.

21. Yao S, Hu K, Tang G, et al. Molecular PET imaging of cyclophosphamide induced apoptosis with 18F-ML-8. *Biomed Res Int*. 2015;2015:317403. doi:10.1155/2015/317403.

22. Blankenberg FG. In vivo imaging of apoptosis. *Cancer Biol Ther*. 2008;7(10):1525–1532.

23. Ashcroft T, Simpson JM, Timbrell V. Simple method of estimating severity of pulmonary fibrosis on a numerical scale. *J Clin Pathol*. 1988;41(4):467–470.

24. du Bois RM. Strategies for treating idiopathic pulmonary fibrosis. *Nat Rev Drug Discov*. 2010;9(2):129–140. doi:10.1038/nrd2958.

25. Nalysnyk L, Cid-Ruzafa J, Rotella P, Esser D. Incidence and prevalence of idiopathic pulmonary fibrosis: review of the literature. *Eur Respir Rev*. 2012;21(126):355–361. doi:10.1183/09059180.00002512.

26. Zhou W, Mo X, Cui W, et al. Nrf2 inhibits epithelial-mesenchymal transition by suppressing snail expression during pulmonary fibrosis. *Sci Rep*. 2016;6:38646. doi:10.1038/srep38646.

27. King TE Jr, Pardo A, Selman M. Idiopathic pulmonary fibrosis. *Lancet*. 2011;378(9807):1949–1961. doi:10.1016/s0140-6736(11)60052-4.

28. Martinez FJ, Chisholm A, Collard HR, et al. The diagnosis of idiopathic pulmonary fibrosis: current and future approaches. *Lancet Respir Med*. 2017;5(1):61–71. doi:10.1016/s2213-2600(16)30325-3.

29. Moore BB, Hogaboam CM. Murine models of pulmonary fibrosis. *Am J Physiol Lung Cell Mol Physiol*. 2008;294(2): L152–L160. doi:10.1152/ajplung.00313.2007.